Electrostatic as well as hydrophobic interactions are important for the association of Cpn60 (groEL) with peptides

Jonathan P. Hutchinson, Timothy C. Oldham, Talal S. H. El-Thaher and Andrew D. Miller*

Department of Chemistry, Imperial College of Science, Technology and Medicine, South Kensington, London, UK SW7 2AY

The interactions of groEL with five *N*-dansyl peptides were investigated by means of a fluorescence binding assay. The peptides studied (B_{amph}, B_{hphil}, A_{amph}, A_{hphil}, N_{amph}) were designed and synthesised as systematic variants of each other in terms of their patterns of charge and hydrophobicity. Fluorescence data were analysed using a fluorescence modified, *y*-reciprocal linearised form of the Benesi–Hildebrand equation which was derived from first principles and verified by theoretical simulations. Under optimal conditions, apparent dissociation constants, K_d, were obtained in the μM range. At physiologically relevant ionic strengths, only two peptides (basic amphiphilic B_{amph} and neutral amphiphilic N_{amph}) interacted with groEL whilst a third peptide (acidic amphiphilic A_{amph}) was able to interact but only at very high ionic strength (> 1 mol kg^{-1}). Thermodynamic (van't Hoff) analysis of the tightest binder, basic amphiphilic B_{amph} peptide, revealed endothermic binding and a large positive entropy, ΔS^{o}_{bind}, consistent with a mixed binding mode involving both hydrophobic and electrostatic interactions. At physiologically relevant ionic strengths, positively charged amino acid residues appear to augment hydrophobic binding interactions with groEL by electrostatic attraction whilst negatively charged amino acid residues oppose short-range hydrophobic interactions with electrostatic repulsion. In conclusion, whilst a principal means of interaction between groEL and a peptide or partially folded protein substrate is certainly hydrophobic, electrostatic effects can modulate or even overwhelm this interaction.

Introduction

Molecular chaperones, according to definition, are proteins whose function is to mediate the folding/refolding of other proteins without becoming part of the final folded structure. Many were first identified as heat shock proteins but most are now known to be constitutively expressed as well. Of all the known molecular chaperones, perhaps the best characterised are the *Escherichia coli* (*E. coli*) molecular chaperone chaperonin 60 (Cpn60; groEL) and its co-molecular chaperone co-chaperonin 10 (Cpn10; groES). Both groEL and groES have been extensively characterised by electron microscopy[1–3] and the X-ray crystal structures of both groEL[4] and groES[5] are now available. As a result, it is now well established that groEL is a homo-oligomer comprising 14 subunits (each 57 259 Da) arranged in two stacked rings of seven subunits each, whilst groES consists of seven subunits (each 10 368 Da) arranged in a single ring. There have been many recent investigations into the way in which groEL and groES mediate protein folding/refolding. These usually involve *in vitro* refolding studies in which a wide variety of different unfolded 'substrate' proteins are refolded in the presence and absence of molecular chaperone and various cofactors, most especially ATP. Unfortunately, the requirements for successful chaperone-assisted refolding appear to vary substantially from one model substrate protein to the next. Moreover, there also appear to be differences in the extent to which the molecular chaperones groEL and groES influence the kinetics of protein refolding depending upon the nature of the unfolded protein substrate and also the refolding conditions. Where refolding rates have been measured, the rate determining rate constants of the productive refolding pathway have been found to be either unchanged, compared to the spontaneous refolding process,[6,7] slightly increased[8] or even substantially reduced.[9] In spite of these variations, two general models of groEL and groES assisted refolding of proteins have been advanced. In the first,[10] groEL and groES are proposed to promote unfolding of misfolded proteins which may then attempt to fold/refold correctly and in the second,[11] the interior cavity of groEL is considered to provide a controlled environment for refolding of the 'substrate' protein at infinite dilution. Doubtless, further research will determine which of these two models most closely describes chaperone-assisted refolding, although the most recent studies reported do not appear to be resolving the issue.[12,13]

Perhaps one of the few readily identifiable, unifying principles of chaperone-assisted folding/refolding of proteins is that an interaction between a partially folded protein substrate and groEL is pivotal to the success of the whole process. This interaction appears to be controlled in extent and strength by changes induced in the quaternary structure of groEL through the binding of ATP and groES,[2,12,14] although how this interaction is brought about and what promotes it is still the subject of some debate. This paper describes some of our recent work directed towards understanding this crucial molecular recognition phenomenon.

Experimental

Materials

All chemicals used were of analytical grade or better and were obtained from Sigma Chemical Co, Poole, Dorset, UK. Deionised distilled MilliQ water was used throughout.

GroEL was purified from a recombinant strain of *E. coli* according to previously published methods.[6,14] After extensive dialysis at 4 °C against 50 mM TRIS-Cl [tris(hydroxymethyl)-methylammonium chloride] buffer (pH 7.6 at ambient temperature) (M = mol dm^{-3}), containing 2 mM 2-mercaptoethanol, groEL was concentrated (10 ml, Amicon stirred cell) over a 100 kDa YM100 membrane to approximately 150 μM (homo-oligomer concentration). GroEL concentrations in stock solutions were determined by quantitative amino acid analysis.

The basic amphiphilic peptide (B_{amph}) with an *N*-terminal 5-dimethylamino-1-naphthalenesulfonyl [dansyl (Dn)] group (see

Fig. 2) and the undansylated basic amphiphilic peptide (NH_2-PLYKKIIKKLLES-OH) were gifts of Roche Products Ltd., Welwyn Garden City, Herts., UK. The other *N*-dansyl peptides [basic hydrophilic peptide (B_{hphil}), acidic amphiphilic peptide (A_{amph}), acidic hydrophilic peptide (A_{hphil}), and neutral amphiphilic peptide (N_{amph}); see Fig. 2] were supplied by Genosys Inc., Cambridge, UK. Concentrated stocks of each *N*-dansyl peptide were prepared in dimethylsulfoxide and stored in aliquots at −70 °C. *N*-Dansyl peptide concentrations were judged spectrophotometrically using an extinction coefficient, ε_{330}, of 4500 dm^3 mol^{-1} cm^{-1} originally measured for dansylglycine. Concentrations of the undansylated basic amphiphilic peptide were determined spectrophotometrically using a tyrosine extinction coefficient, ε_{280}, of 1280 dm^3 mol^{-1} cm^{-1}.[15]

Simulations were performed on a Power Macintosh 6100/60 using the Markov 4.0.3 Kinetics Simulator software package (Ralph Sutherland, Scientific Software, 1994). UV–VIS absorption measurements were made on a Pharmacia LKB Ultrospec III at room temperature. Fluorescence assays were performed on a Shimadzu RF 5001PC spectrofluorophotometer, fitted with a thermostatted cuvette holder, using monochromator band-widths of 5 nm.

Fluorescence assay

All fluorescence assays were carried out in an assay buffer of 50 mM TRIS-Cl, containing 2 mM 2-mercaptoethanol, which was adjusted to pH 7.6 at the desired assay temperature. For each peptide, a stock solution (100 μM) in assay buffer was made up after which an aliquot was transferred to a fluorescence cuvette (10 mm pathlength) where it was diluted to a final concentration of 3 μM in assay buffer (1 ml). After 10 min thermal equilibration using a water bath set at the desired assay temperature, the peptide solution in the cuvette was titrated with groEL from a homo-oligomer concentration of 10 nM up to 3 μM (typically in 18 stages). After each stage of addition, the solution in the cuvette was mixed thoroughly, thermally equilibrated for 2 min (as above) and then the fluorescence emission spectrum recorded at 450–600 nm, using an excitation wavelength of 350 nm. Longer equilibration times did not affect the results. Each aliquot addition of groEL was made from one of three stock solutions of the homo-oligomer (*i.e.* 15, 75 or 154 μM homo-oligomer concentration in assay buffer), using a 10 μl syringe (Hamilton), so as to keep the aliquots small. For each assay, an identical control experiment was always performed in the absence of peptide so as to evaluate the contribution of groEL alone to the fluorescence spectrum. This contribution was subtracted from the corresponding spectrum recorded in the presence of peptide prior to processing of the data. For binding assays performed at increasing ionic strength, a stock solution of ammonium sulfate or magnesium chloride (each 4 M) in assay buffer was made up after which appropriate aliquots were added to the fluorescence cuvette. Binding assays performed with proteins other than groEL were carried out in a similar way. Human serum albumin (HSA) concentrations were determined using an $A_{280}^{1\%}$ of 5.3 and a molecular mass of 69 000 Da.[16]

Fluorescence emission intensities at 500 nm, corrected for groEL background, were tabulated and the emission intensity of free peptide at 500 nm (*i.e.* in the absence of groEL) was subtracted in order to give the fluorescence intensity enhancement, ΔI_{500}, due to interaction of the given peptide with groEL at each individual groEL concentration. ΔI_{500} data were then analysed using a model for binding in which a given peptide was assumed to be able to interact with an unspecified number of independent binding sites on the groEL homo-oligomer. This model was used to derive expression (1), a fluorescence modification of the Benesi–Hildebrand eqn. (1)[17] where $[P]_t$ is the total peptide concentration, $[G]_t$ the total groEL concentration, ΔI_{500} the fluorescence intensity enhancement at 500 nm, K_a the apparent association constant and $\Delta\Phi$ a term deriving from fluorescence quantum yield enhancement upon peptide binding to groEL. The origins of these terms and the theoretical basis of the model are discussed in the following section.

$$[P]_t[G]_t/\Delta I_{500} = 1/K_a\Delta\Phi + [G]_t/\Delta\Phi \quad (1)$$

Theory

The interaction of groEL with a protein is likely to be an extremely complex phenomenon. In order to probe this interaction we chose to use short peptide chains, rather than large proteins, enabling us to assume reasonably that each peptide interacts with only one potential binding site on the groEL macromolecule. There are probably still a range of binding sites on groEL with potentially different affinities for each peptide. Nevertheless, we chose to devise a simple model binding scheme, based on a number of simplifying assumptions, with which to analyse binding data. The first assumption, already alluded to, was that each peptide molecule (P) is able to bind to only one groEL molecule (G) at any one time and that each groEL molecule may bind up to *n* peptide molecules in *n* discrete, independent binding sites.

The chosen fluorescence binding assay (see below) depends on the measurement of spectral changes occurring when a fluorescent peptide moves from an aqueous, highly polar and unconstrained environment to a different, possibly less polar, possibly more constrained environment upon association with groEL. There may well be slight polarity and rigidity differences between binding sites, but in steady state studies such as these, the contribution of such effects to the overall shift is likely to be minimal. These considerations lead to the second assumption that spectroscopic differences between sites are not resolvable at the assay resolution (*i.e.* the *n* peptide binding sites are essentially spectroscopically indistinguishable one from another). Significant spectroscopic differences are likely to be associated with differences in affinities for different sites, and tests for this are described and the results discussed below. The third assumption was that trimolecular and higher order processes contribute negligibly to the overall binding scheme which may then be expressed as a simple series of binding equilibria, (Scheme 1), where the stepwise binding constant, $K_{a,i}$ for a

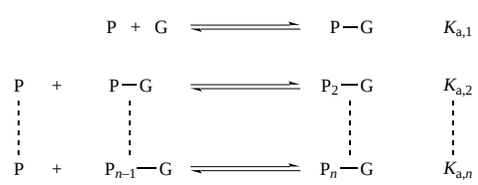

Scheme 1

general step *i* (*i* is an integer between 1 and *n*) may be given in the form $K_{a,i} = [P_i–G]/([P][P_{i-1}–G])$.

The following derivation is based upon the treatments of Benesi and Hildebrand[17] and Connors.[18] The interaction of P with any single binding site G′ may be described by a microscopic association constant κ_a, eqn. (2).

$$\kappa_a = ([P–G']/([P][G']) \quad (2)$$

If a fourth assumption is made that each individual binding site (G′) has approximately equal affinity for peptide (*i.e.* the distribution of affinities is narrow), then $K_{a,i}$ and κ_a may be related by expression (3): noting especially that $K_{a,1} = n\kappa_a$. This

$$K_{a,i} = [n - (i - 1)]\kappa_a/i \quad (3)$$

assumption does not prevent peptides of different hydrophilicity

accessing different types of binding sites but it does restrict the access of peptides to only a narrow distribution of types. In order to derive an equation to analyse fluorescence data, an expression for [P–G′] is required. The extent of binding (χ) of peptide to groEL is defined, somewhat unconventionally, as the fraction of total P bound to G which can be written as eqn. (4),

$$\chi = [\text{P–G}']/[\text{P}]_t \quad (4)$$

where $[\text{P}]_t$ corresponds to the total concentration of peptide both unbound and bound to groEL. This definition is required because groEL, with its many binding sites, was titrated against a fixed concentration of fluorescent peptide. We may write eqn. (5). By combining expressions (2), (4) and (5), the extent of

$$[\text{P}]_t = [\text{P}] + [\text{P–G}'] \quad (5)$$

binding (χ) may be rewritten as eqn. (6). Expressions (4) and

$$\chi = \kappa_a[\text{G}']/(1 + \kappa_a[\text{G}']) \quad (6)$$

(6) may now be combined and solved for [P–G′], eqn. (7).

$$[\text{P–G}'] = [\text{P}]_t\kappa_a[\text{G}']/(1 + \kappa_a[\text{G}']) \quad (7)$$

We now consider the fluorescence emission from a solution of *N*-dansyl peptide and groEL. If a fifth assumption is made that groEL neither absorbs significantly at the excitation wavelength nor fluoresces significantly (valid for our experimental assay), then the fluorescence intensity at a given emission wavelength, I_F, is described by eqn. (8), where I_o is the intensity of

$$I_F = \Phi_t\varepsilon_t I_o \Delta l [\text{P}]_t \quad (8)$$

excitation light within the depth Δl of solution imaged by the fluorimeter, and ε_t and Φ_t are respectively the extinction coefficient (at the excitation wavelength) and the fluorescence quantum yield (at the given emission wavelength)‡ of the peptidyl dansyl group. Both ε_t and Φ_t are averaged over all environments and will therefore vary with χ. I_o can be regarded as constant (and contributions due to reabsorption of fluorescence negligible) when the optical density of the groEL/peptide solution, measured at excitation and emission wavelengths, is maintained below approximately 0.05 throughout an experiment. Expression (8) may therefore be simplified to eqn. (9), where $\boldsymbol{\Phi}_t = \Phi_t\varepsilon_t$

$$I_F = \boldsymbol{\Phi}_t I [\text{P}]_t \quad (9)$$

and $I = I_o\Delta l$. In the absence of groEL, expression (9) becomes eqn. (10), where $\boldsymbol{\Phi}_P = \Phi_P\varepsilon_P$ (ε_P and Φ_P being the extinction co-

$$I_F = \boldsymbol{\Phi}_P I [\text{P}]_t \quad (10)$$

efficient and fluorescence quantum yield of the peptidyl dansyl group free in solution). In the presence of groEL, expression (9) may be expanded, using the additional relationship $\boldsymbol{\Phi}_{P–G'} = \Phi_{P–G'}\varepsilon_{P–G'}$ ($\varepsilon_{P–G'}$ and $\Phi_{P–G'}$ being the extinction coefficient and fluorescence quantum yield of the peptidyl dansyl group bound to groEL), to eqn. (11).

$$I_F = \boldsymbol{\Phi}_P I\,[\text{P}] + \boldsymbol{\Phi}_{P–G'} I[\text{P–G}'] = \boldsymbol{\Phi}_P I[\text{P}]_t + \{\boldsymbol{\Phi}_{P–G'} - \boldsymbol{\Phi}_P\} I\,[\text{P–G}'] \quad (11)$$

Note now that $\boldsymbol{\Phi}_P$ and $\boldsymbol{\Phi}_{P–G'}$ are independent of χ. The change in fluorescence intensity on peptide binding to groEL, ΔI_F, is now simply the difference between expressions (11) and (10), eqn. (12), where $\Delta\boldsymbol{\Phi} = \{\boldsymbol{\Phi}_{P–G'} - \boldsymbol{\Phi}_P\}I$, which can now be

$$\Delta I_F = \Delta\boldsymbol{\Phi}[\text{P–G}'] \quad (12)$$

regarded as the enhancement of the dansylpeptide fluorescence quantum yield on binding. Combining expression (7) with (12), yields eqn. (13). We cannot determine [G′] from experimental

$$\Delta I_F = \Delta\boldsymbol{\Phi}[\text{P}]_t\kappa_a[\text{G}']/(1 + \kappa_a[\text{G}']) \quad (13)$$

fluorescence data. However, by making the approximation that the concentration of peptide-free groEL binding sites, [G′], is a product of the total number of binding sites *n* and the total concentration of groEL, $[\text{G}]_t$, then binding parameters may then be extracted using the following *y*-reciprocal linearisation, eqn. (14). By plotting the left hand side of eqn. (14) against $[\text{G}]_t$,

$$\frac{[\text{P}]_t[\text{G}]_t}{\Delta I_F} = 1/(n\kappa_a\Delta\boldsymbol{\Phi}) + [\text{G}]_t/\Delta\boldsymbol{\Phi} \quad (14)$$

a constant $n\kappa_a$ may be obtained from the ratio of slope and intercept. This constant, which is equivalent to $K_{a,1}$, represents an apparent association constant which we denote K_a in the remainder of the paper. The reciprocal is the apparent dissociation constant which we denote K_d. By substituting K_a for $n\kappa_a$ and defining the fluorescence emission wavelength to be 500 nm, expression (1) (see above) results.

Theoretical simulations

Simulations were performed to test the validity of the approximation $[\text{G}'] = n[\text{G}]_t$. Separate simulations were performed assuming a total number of $n = 4$, 10 and 15 independent, equal affinity peptide binding sites. A series of *n* single peptide binding equilibria were then assumed with equilibrium association constants $K_{a,i}$ ($i = 1–n$). The simulator requires rate constants rather than equilibrium constants. Therefore, the ratio of forward to reverse rate constants, $K_{a,i}$, was calculated using expression (3) and $n\kappa_a = 1.6\ \mu\text{M}^{-1}$ (apparent $K_d = 0.625\ \mu\text{M}$, corresponding closely to experimentally determined values) and magnitudes of forward and reverse rate constants were determined by setting the larger value to the largest numerical value which the simulator will accept. For all the simulations, initial peptide and groEL concentrations were entered and the endpoint established when species concentrations were changing by at most 0.01% every 10 iterations. Values of ΔI_F were then calculated from eqn. (13) assuming $\Delta\boldsymbol{\Phi}$ to be $70\ \mu\text{M}^{-1}$ (similar to experimentally determined values) and using equilibrium values of [G′] obtained from the simulator. Fig. 1 shows the results of the $n = 10$ simulation plotted using a *y*-reciprocal form of expression (13) (the 'exact' solution) and expression (14) (the 'experimental' solution). The linearity of the 'exact' data set confirms that expression (13) correctly describes the proposed binding model. The 'experimental' solution is essentially indistinguishable from the 'exact' solution for $n[\text{G}]_t > [\text{P}]_t$. For lower values of $[\text{G}]_t$, the plot departs from linearity as the approximation that $[\text{G}'] = n[\text{G}]_t$ breaks down. However, Fig. 1 demonstrates that the 'experimental' solution may still be used to derive measured binding parameters provided that sufficient fluorescence data is acquired (*i.e.* >70% of saturation[18]). In that event, linear regression analysis of the 'experimental' solution (neglecting data points deviating significantly from linearity at low $[\text{G}]_t$) will give binding parameters within 20% of the actual values, with the error falling as *n* increases. The results of other simulations, where $n = 4$ or 15 and where $[\text{P}]_t$ was varied, gave very similar plots to those shown in Fig. 1.

Simulations were also performed to investigate how far departures from the model could take place before distortions became manifest in the data analysis. We found that cooperative binding gave a very similar shaped reciprocal plot to the independent site model described above, including the curv-

‡ Though a quantum yield measurement conventionally applies to the total integrated emission, it is possible to regard a species as having a quantum yield for emission at a particular wavelength. In this work, Φ_t is the product of the total fluorescence quantum yield and the fraction of the emission envelope imaged at the chosen emission wavelength.

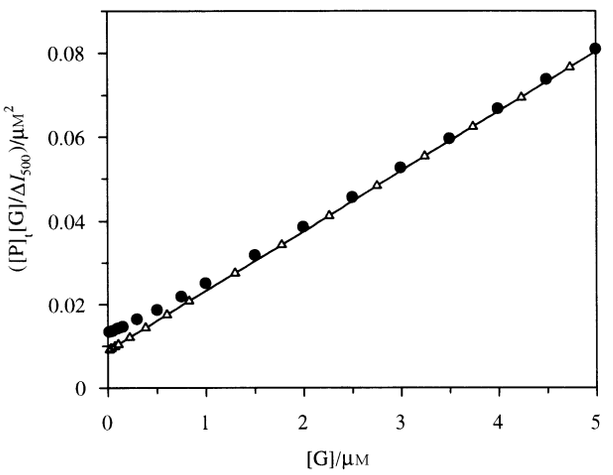

Fig. 1 Simulated fluorescence assay. Simulated binding assay, for the case where $[P]_t = 3$ μM and $n = 10$, generated using the Markov 4.0.3 Kinetics Simulator as described in the text. Simulated fluorescence data are plotted using a *y*-reciprocal linearisation of expression (13) (Δ) (where [G] corresponds to [G′]) or expression (14) (●) (where [G] corresponds to $[G]_t$) incorporating the approximation $[G'] = n[G]_t$. The first mentioned plot (Δ) has been multiplied by 1/*n* so that the abcissae scales are comparable.

ature observed at low groEL concentrations (see Fig. 1). However, cooperativity was found to be reflected in a value of K_a which was higher than that obtained from the independent site model and which was no longer equal to $K_{a,1}$. For instance, when $K_{a,i}$ was assumed to increase by a factor of $2^{(i-1)}$ over the independent site value, in an $n = 4$ simulation, K_a increased to 1.01 from 0.4 μM^{-1} although $K_{a,1}$ was the same in both cases. Cooperativity was detectable in a plot of ΔI_F against $[G]_t$. In the independent site case, this plot was a rectangular hyperbola (slightly distorted by the approximation $[G'] = n[G]_t$), while in the cooperative case it was sigmoidal at very low groEL concentrations. Connors[18] points out that the curve only becomes sigmoidal given a certain level of cooperativity (*i.e.* when $2K_{a,2} > K_{a,1}$ a sigmoidal curve is guaranteed for all *n*, but other conditions are sufficient where $n > 2$) and that for weaker cooperativity the isotherm simply departs from the rectangular hyperbola. Rigorous analysis of models with a range of different affinity sites was beyond the Markov simulator, but simple simulations performed where site affinities were substantially different (tenfold) were able to show that reciprocal plots ceased to be linear. Connors[18] also describes how the curvature of reciprocal plots may be a signature for multiple affinity equilibria. In conclusion, these simulations indicated that *y*-reciprocal linearisation data analysis of fluorescence binding data would not necessarily characterise departures (in the form of small cooperativity effects and small distributions in microscopic binding constants, $K_{a,i}$) from the independent site, equal affinity model described above. Other graphical tests would therefore be required to test more rigorously for departures from the model (see Discussion section).

Results

Peptide Sequences

The interaction of five different peptides with groEL was investigated. The sequence alignment of these five peptides (Fig. 2) illustrates the relative dispositions of charged and hydrophobic amino acid residues. Thus, the basic amphiphilic (B_{amph}) peptide alternated pairs of positively charged lysine (K) residues with hydrophobic isoleucine (I) and leucine (L) residues, the acidic amphiphilic (A_{amph}) peptide pairs of negatively charged glutamate (E) residues with hydrophobic (I and L) residues and the neutral amphiphilic (N_{amph}) peptide pairs of neutral glutamine (Q) residues with hydrophobic (I and L) residues. In the event that any of these three sequences were to

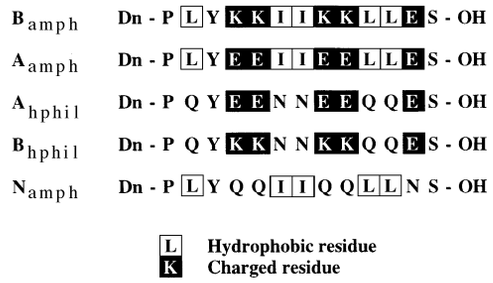

Fig. 2 Sequence summary of five *N*-dansylpeptides. Single letter amino acid code has been used throughout to denote amino acid residues. The abbreviations are: proline, P; leucine, L; tyrosine, Y; lysine, K; isoleucine, I; glutamic acid, E; serine, S; glutamine, Q; asparagine, N. Each peptide has an *N*-terminal 5-dimethylamino-1-naphthalenesulfonyl [Dansyl (Dn)] group acting as an environment sensitive fluorophore.

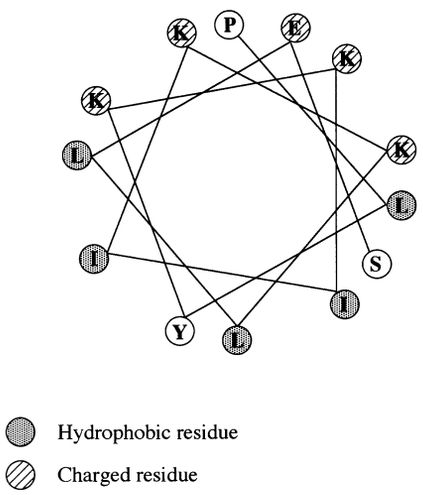

Fig. 3 Helical wheel diagram of the B_{amph} peptide

adopt an α-helical conformation, then an amphiphilic α-helix would result as shown by the helical wheel diagram (Fig. 3) of the B_{amph} peptide. By contrast, the basic hydrophilic (B_{hphil}) and acidic hydrophilic (A_{hphil}) peptides alternated positively charged lysine (K) residues or negatively charged glutamate (E) residues respectively with polar neutral asparagine (N) or glutamine (Q) residues. All the peptides were charged with a dansyl group to act as a fluorescent reporter.

Fluorescence binding assays

Typically, assays were carried out with the following results. Excitation of the *N*-dansyl peptides in free solution at 350 nm resulted in a weak fluorescence emission maximum at *ca.* 540 nm. Upon titration with groEL, the binding interaction was characterised by a blue shift in the emission maximum towards 500 nm and an increase in fluorescence intensity which tended towards saturation with increasing groEL concentration [Fig. 4(*a*)]. In the absence of interaction, as observed when dansylglycine was titrated with groEL (see below), no such blue shift and fluorescence intensity increase was observed. The extent of the binding interaction was assessed by plotting the fluorescence intensity enhancement at 500 nm, ΔI_{500}, corrected for groEL background, against groEL concentration [Fig. 4(*b*)] and then transposing this data into a linear form [Fig. 4(*c*)] using expression (1). From this transposition, the apparent association constant, K_a, was determined by dividing the plot gradient by the intercept. Typically, final groEL concentrations were not increased above 3 μM (total absorbance at 350 nm < 0.07 AU) to prevent fluorescence reabsorption and inner-filter effects. Therefore, apparent association constants below

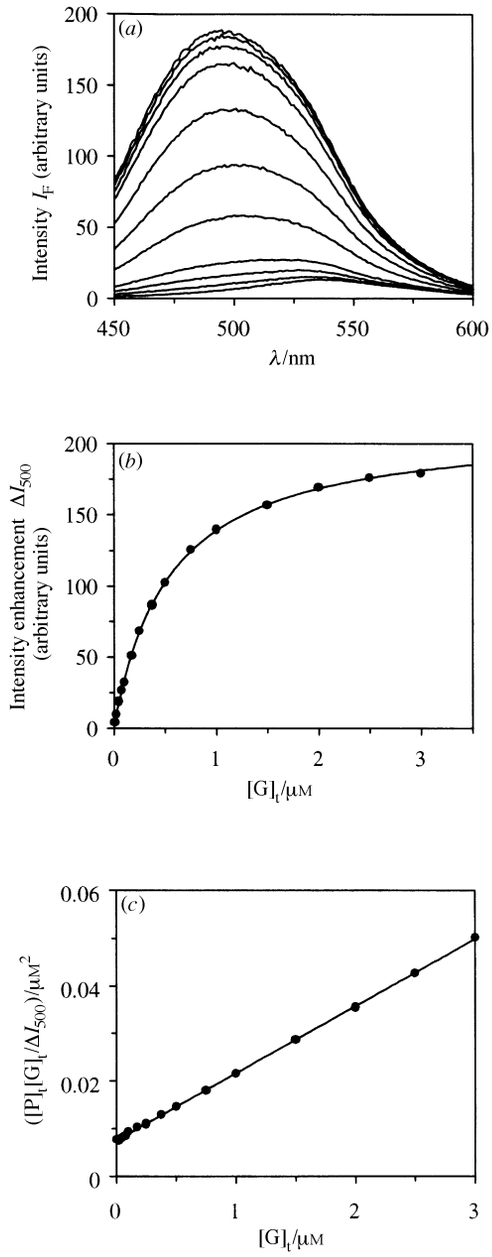

Fig. 4 Fluorimetric binding assay–groEL *vs.* fixed concentration of B_{amph} peptide. (*a*) The Figure shows the increase in fluorescence intensity and blue-shift observed when a solution of the fluorescent *N*-dansyl B_{amph} peptide (3 μM), at 20 °C in a buffer of 50 mM TRIS-Cl (pH 7.6) containing 2 mM 2-mercaptoethanol, was titrated with groEL. GroEL concentrations were increased stepwise from 10 to 3000 nM (homo-oligomer concentration). A series of representative fluorescence spectra are shown. Fluorescence excitation was performed at 350 nm, with excitation and emission band widths of 5 nm. The contribution of groEL to the observed spectra has been subtracted in each case; (*b*) Binding isotherm. In order to analyse the fluorescence data for binding information, the increase in fluorescence intensity at 500 nm, ΔI_{500}, was plotted as a function of groEL concentration. The binding isotherm shown was plotted from the data shown in Fig 4(*a*) and the best-fit line is a simple hyperbolic function; (*c*) Derivation of K_a and K_d. Fluorescence binding isotherms were linearised with expression (1) to give plots from which dissociation constants (K_d) could be calculated as the ratio of intercept to gradient. The plot shown was obtained by processing the data shown in 4(*b*). Data were fitted by least-squares analysis with simple weighting.

10^5 M^{-1} (corresponding to apparent dissociation constants K_d of above 10 μM) could not be measured.

Table 1 shows a series of groEL binding data, expressed as K_d values, obtained at 20 °C with all five peptides in the standard 50 mM TRIS-Cl, pH 7.6, 2 mM 2-mercaptoethanol assay buffer. Binding interactions were examined not only with groEL but

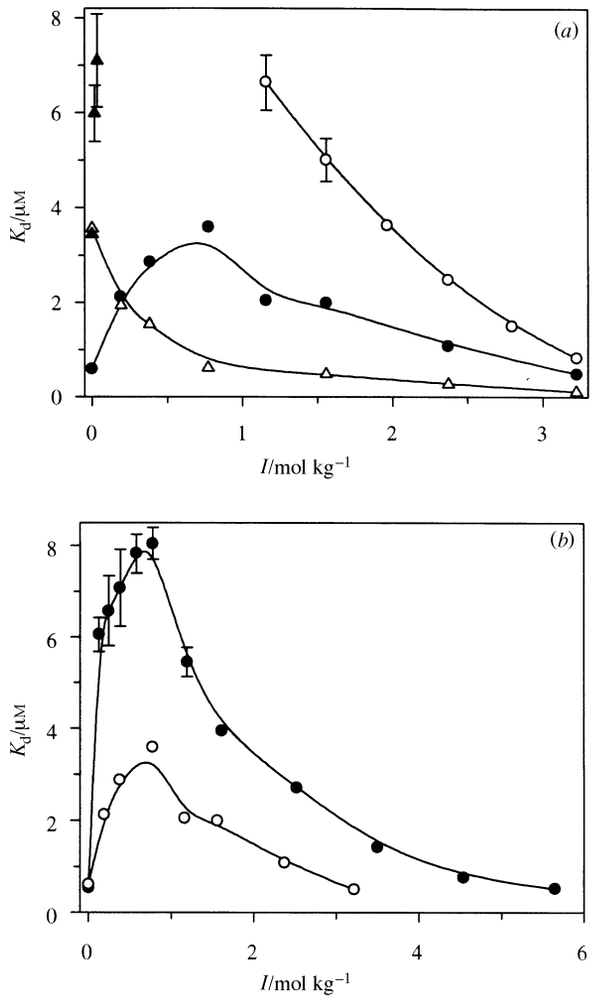

Fig. 5 Effect of ionic strength on K_d. (*a*) Binding assays were performed at 20 °C in 50 mM TRIS-Cl (pH 7.6), 2 mM 2-mercaptoethanol. For each peptide (Fig. 2) separate fluorimetric binding assays were conducted at the indicated ionic strengths, *I*, defined by increasing concentrations of $(NH_4)_2SO_4$. The variation in K_d of the B_{amph} (●), A_{amph} (○), N_{amph} (△) and B_{hphil} (▲) peptides was plotted as a function of *I* as shown. Error margins were derived from the standard errors of the linearised binding isotherm plots (Fig. 4) and are shown where these are larger than the point size. The best-fit lines through the data are spline functions. (*b*) Salt effects on K_d. Comparison of the effect of $(NH_4)_2SO_4$ (○) or $MgCl_2$ (●) on the variation of K_d with ionic strength as measured for the B_{amph} peptide.

also with human serum albumin (HSA), lysozyme and DNase. In the latter instances, all three proteins could be titrated to higher concentrations than groEL before absorption became excessive, therefore K_d values up to 50 μM were measurable. Also included in Table 1 are results of control experiments performed with dansylglycine in place of the *N*-dansyl peptides.

The effect of ammonium sulfate, $(NH_4)_2SO_4$, ionic strength on the interaction of all five *N*-dansyl peptides with groEL was investigated and is summarised in Fig. 5(*a*) where the binding interaction, measured in terms of K_d, is plotted as a function of ionic strength, *I*. For comparison, the effect of magnesium chloride, $MgCl_2$, ionic strength on the interaction of the B_{amph} peptide with groEL was also investigated as shown in Fig. 5(*b*). In the cases of both salts, molarity concentrations (mol dm^{-3}) were converted to molalities (mol kg^{-1}), using experimentally derived calibration curves, to enable calculation of the ionic strength, *I*.

Finally, the effect of temperature on the binding of the *N*-dansyl peptides to groEL was investigated. The results obtained [over the temperature range 10–42 °C (*i.e.* 283–315 K)] are shown in the form of van't Hoff plots (Fig. 6) where K_a are used

Table 1 Apparent dissociation constants, K_d, for peptide–protein binding. Peptide–protein dissociation constants, K_d (μM), were determined at 20 °C in 50 mM TRIS-Cl (pH 7.6), 2 mM 2-mercaptoethanol, by the standard fluorimetric binding assay (Fig. 4) described in the text. Peptide sequences are given in Fig. 2.

	B_{amph}	A_{amph}	A_{hphil}	B_{hphil}	N_{amph}	Dn-Gly
groEL	0.54 ± 0.01	*a* (0.83 ± 0.02)[d]	*a*	3.44 ± 0.13	3.57 ± 0.19	*a*
HSA	31.6 ± 0.8	3.83 ± 0.2 (10.0 ± 0.5)[d]	29.0 ± 0.3	*b*	29.9 ± 5.1	3.5 ± 0.3 [2.2][c]
Lysozyme	*b*	*b*	*b*	*b*	*b*	*b*
Dnase	*b*	*b*	*b*	*b*	*b*	*b*

[a] Not measurable (K_d > 10 μM). [b] Not measurable (K_d > 50 μM). [c] Ref. 16. [d] Assay performed in the presence of 1 M $(NH_4)_2SO_4$

Table 2 Thermodynamic parameters for peptide/groEL interaction. Binding assays were performed over a range of temperatures with each peptide in 50 mM TRIS-Cl (pH 7.6), 2 mM 2-mercaptoethanol (in the optional presence of 1 M $(NH_4)_2SO_4$ as indicated). At each temperature a standard fluorimetric binding assay was performed to determine K_a. Thermodynamic data were obtained by van't Hoff analysis [Fig. 6(*a*)] of each complete set of temperature-dependent K_a values. Peptide sequences are given in Fig. 2.

	B_{amph}	A_{amph}[a]	A_{hphil}	B_{hphil}[b]	N_{amph}
ΔH°_{bind}/kJ mol^{-1}	67.5 ± 7.9	5.5 ± 2.8	*c*	50.2 ± 9.3	0.48 ± 5.7
ΔS°_{bind}/J K^{-1} mol^{-1}	351 ± 27	134 ± 9	*c*	269 ± 31	107 ± 20
ΔG(37 °C)$_{bind}$/kJ mol^{-1}	−41.3 ± 11.5	−36.2 ± 6.2	*c*	−33.2 ± 13.3	−32.9 ± 8.5

[a] Assays performed in the presence of 1 M $(NH_4)_2SO_4$. [b] Temperature: 30–42 °C. [c] Not measurable (K_d > 10 μM).

Table 3 Thermodynamic parameters for interaction of B_{amph} peptide with groEL at increasing ionic strength. Binding assays were performed over a range of temperatures in 50 mM TRIS-Cl (pH 7.6), 2 mM 2-mercaptoethanol and in the presence of three different concentrations of $(NH_4)_2SO_4$ corresponding to three different ionic strengths as shown in the Table. At each temperature a standard fluorimetric binding assay was performed to determine K_a. The complete set of temperature-dependent K_a values, for a given ionic strength, were processed by van't Hoff analysis [Fig. 6(*b*)] to provide the thermodynamic data described in the Table. Data for binding at zero ionic strength are taken from Table 2 and shown for comparison.

	Ionic strength			
	0	0.19	1.16	3.22
ΔH°_{bind}/kJ mol^{-1}	67.5 ± 7.9	14.4 ± 5.8	15.7 ± 3.7	8.2 ± 2.8
ΔS°_{bind}/J K^{-1} mol^{-1}	351 ± 27	156 ± 19	159 ± 12	150 ± 9
ΔG(37 °C)$_{bind}$/kJ mol^{-1}	−41.3 ± 11.5	−34.0 ± 8.3	−33.7 ± 5.3	−38.2 ± 4.0

in place of K_d values as a measure of binding ability. Assays were performed either in the absence of added salt or in the presence of $(NH_4)_2SO_4$ to make up the ionic strength. Thermodynamic parameters were then derived using eqns. (15) and (16), where ΔH°_{bind} is the standard enthalpy for peptide binding

$$\ln K_a = -\Delta H^\circ_{bind}/RT + \Delta S^\circ_{bind}/R \quad (15)$$

$$\Delta G(T)_{bind} = \Delta H^\circ_{bind} - T\Delta S^\circ_{bind} \quad (16)$$

(under the conditions of pH, ionic strength, ambient pressure and fixed peptide concentration used in the binding assays), ΔS°_{bind} the standard entropy, $\Delta G(T)_{bind}$ the temperature dependent free energy change of binding and R the molar gas constant (8.314 J mol^{-1} K^{-1}). Tables 2 and 3 summarise the thermodynamic data calculated from the van't Hoff plots. Owing to the extremely weak binding behaviour of the A_{hphil} peptide it proved impossible to determine any thermodynamic parameters for the binding of this peptide with groEL.

Discussion

The theoretical basis underpining the fluorescence binding assay described above is that when a fluorophore attached to a ligand experiences a change of environment as a result of ligand binding, then this is accompanied by a change in fluorescence quantum yield and emission maximum.[16,19] Therefore, it was anticipated that changes in the fluorescence behaviour of the *N*-dansyl group attached to the five peptide sequences, shown in Fig. 2, would allow information on the interaction of the peptides with groEL to be established. The five peptide sequences investigated were designed on the basis of experimental data, published when these investigations began, which established the importance of hydrophobic amino acids as well as the possibility that basic amphiphilic α-helices may be crucial recognition elements.[20] The first sequence synthesised was the B_{amph} peptide which was designed as a potential amphiphilic α-helix forming peptide (Fig. 3). The remaining four peptides were designed and synthesised as systematic variants in the pattern of charge and hydrophobicity relative to the B_{amph} peptide.

A major problem was encountered immediately a fluorescence binding assay between the B_{amph} peptide and groEL was attempted. When peptide was titrated against a fixed homo-oligomer concentration of groEL (100 nM) a fluorescent intensity enhancement and a blue shift were observed suggesting that peptide binding was occurring (results not shown). However, even at a peptide concentration of 12.5 μM (peptide : homo-oligomer mol ratio of 125 : 1) there appeared no sign of fluorescence saturation. This is almost certainly due to the high stoichiometry of peptide binding to groEL. However, this presented problems since at higher peptide concentrations self-association induced fluorescence enhancement started to become significant and the solution absorbance at the excitation wavelength was already exceeding 0.05 AU beyond which reabsorption and inner filter effects could not be ignored (see Results section). Therefore, in order to bring about fluorescence saturation under conditions where peptide self-association and reabsorption/inner filter effects could be ignored, we chose to maintain the peptide concentration constant (at 3 μM) whilst titrating with groEL instead. In this case, fluorescence saturation could indeed be achieved [Figs. 4(*a*) and 4(*b*)] and fluorescence data obtained proved amenable to analysis using expression (1) giving a linear plot [Fig. 4(*c*)] from which an apparent association (K_a) and dissociation (K_d) constant could be derived using linear regression analysis with simple weighting. In order to obtain accurate determinations of K_a and K_d, groEL titrations were always made to a point where at least

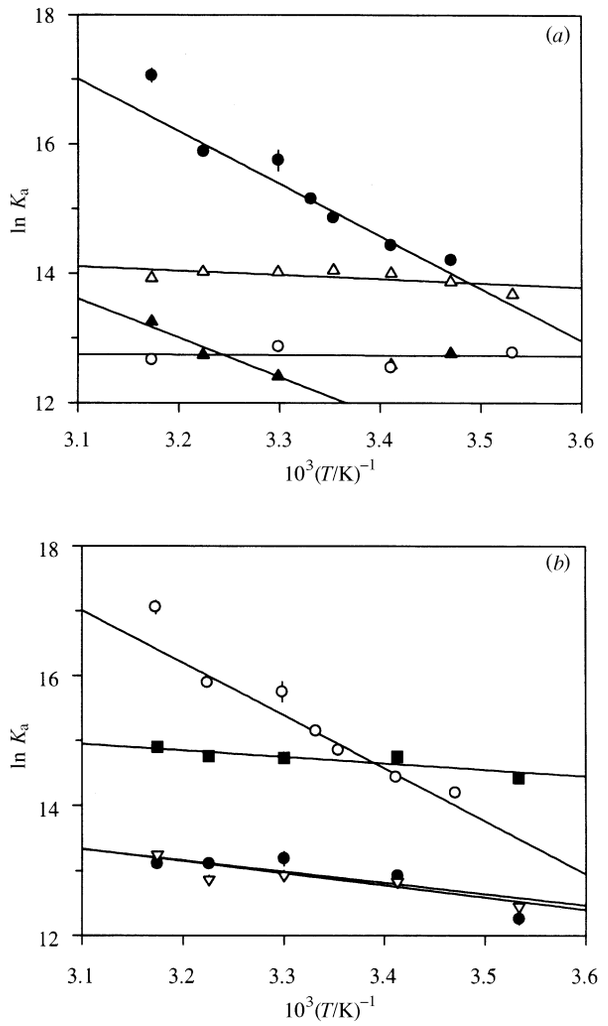

Fig. 6 Effect of temperature on K_a (*a*) For the B_{amph} (●), A_{amph} (△), N_{amph} (○) and B_{hphil} (▲) peptides (Fig. 2), separate fluorimetric binding assays were performed in 50 mM TRIS-Cl (pH 7.6), 2 mM 2-mercaptoethanol, at the indicated temperatures. The variation of K_a with temperature was represented as van't Hoff plots to enable thermodynamic parameters to be deduced (Table 2). Error margins are shown where these are larger than the point size. The error in each point was used to weight the linear fit explicitly; (*b*) Effect of ionic strength and temperature on the K_a of B_{amph}. Three separate sets of fluorimetric binding assays were carried out at the indicated temperatures with the B_{amph} peptide in 50 mM TRIS-Cl (pH 7.6), 2 mM 2-mercaptoethanol, in the presence of 0.0625 M (●), 0.375 M (▽) or 1 M $(NH_4)_2SO_4$ (■). The variation of K_a with temperature was represented as before. Data obtained in the absence of $(NH_4)_2SO_4$ (○) were taken from Fig. 6(*a*).

70% fluorescence saturation was achieved since this is known to be a necessary prerequisite to confirm that a curve is a rectangular hyperbola.[18] The illustrated linear plot [Fig. 4(*c*)] shows a slight deviation from linearity at low groEL concentrations {not fully resolved in [Fig. 4(*c*)]} which was found to be a common feature of such plots. Theoretical simulations using expression (14), from which (1) derives, had shown (Fig. 1) very similar deviations which arose from a breakdown in the approximation $[G'] = n[G]_t$ (*i.e.* that the concentration of available groEL binding sites, [G′], is a product of the total number of binding sites n and the total concentration of groEL, $[G]_t$) under conditions where $n[G]_t < [P]_t$. Presumably, the same explanation holds true for observed deviations from linearity in the experimental data. Fortunately, our theoretical simulations demonstrated (Fig. 1) that non-linear deviations at low $[G]_t$ could be neglected, in fitting the data by linear regression analysis, without introducing significant error into calculations of the binding parameters. The importance of the *y*-reciprocal linearisation then becomes clear since a double reciprocal form of expression (1),[17] involving $1/[G]_t$, would place undue weight on the least reliable data points during regression analysis.

It is useful to emphasise what the assay was achieving, especially since the titrations were performed in a necessarily unconventional way. Saturation in this assay was occurring not when the capacity of groEL for a given peptide was reached, but when the concentration of groEL was such that there was no unbound peptide remaining in the medium. Statistically (for any case where the number of peptide binding sites $n > 1$) this means that any given groEL molecule had at most one bound peptide and therefore the binding isotherm reflected the interaction of this one peptide with groEL. The apparent association constant, K_a, (which characterises this interaction) was found to correlate mathematically (see Theory section) with the first equilibrium constant, $K_{a,1}$, for the interaction of peptide with groEL. This correlation breaks down when binding cooperativity and multiple affinity equilibria exist (as described in the Theory section). Therefore as recommended by Connors,[18] a series of graphical tests were carried out with raw binding data so as to check the validity of the binding model and also, therefore, the correlation between K_a and $K_{a,1}$. This was especially important since theoretical simulations had indicated that small departures from the independent site, equal affinity binding model would not necessarily be apparent using the *y*-reciprocal linearisation analysis (described above) of the fluorescence binding data.

The question of cooperativity was addressed by examining ΔI_{500} *vs.* $[G]_t$ binding isotherms of the type shown [Fig. 4(*b*)]. Through the use of data simulations (see Theory section), such isotherms were found to adopt the form of a rectangular hyperbola in the absence of cooperative binding but acquire sigmoidal character at low groEL concentrations, $[G]_t$, provided cooperative binding was strong enough. Detection of weaker cooperativity was more difficult, particularly since the assumption $[G'] = n[G]_t$ appeared to cause a slight departure from the rectangular hyperbola at low $[G]_t$ anyway. In any event, raw binding data taken from the interaction of peptides (Fig. 2) with groEL were fitted with rectangular hyperbola functions and the residuals examined for systematic variations indicative of cooperativity. In each case, sufficiently low concentrations of groEL were used to enable sigmoidal behaviour to be detected if present. Cooperativity was not observed in any of these plots implying that it must be either weak or absent. This suggests that even if cooperative binding were present but undetectable in the ΔI_{500} *vs.* $[G]_t$ plot, the distortions it introduced to the calculated values of K_a were within experimental error. It should be noted that values for n could not be extracted from rectangular hyperbolic function fits since the assay titrates to excess groEL; 'saturation' therefore does not reflect the capacity of the protein for the peptide [*N.B.* rearrangement of expression (1) shows that the hyperbolic form of the isotherm yields $P_t\Delta\Phi$ and K_a, but not n explicitly].

The question of the existence of multiple affinity equilibria was addressed using the matrix graphical treatment of Coleman *et al.*[21] This treatment is used to identify the number of species in a mixture contributing to a given set of spectrophotometric data. In the case of our fluorescent peptides, if approximately equal affinity equilibria exist, then only two species should contribute to the data set, *i.e.* peptide free in solution and spectroscopically unique peptide bound to any one of the groEL binding sites. When we tested for two contributing species to the observed fluorescence spectra of the B_{amph} peptide, restricting the stoichiometry so that the total concentration of fluorescent species remained constant, the resulting plots (using data covering the full range of groEL concentrations) were linear and passed through the origin ($r > 0.992$ over 21 points; median intercept = 0.1 ± 0.7 over 10 data sets tested) (results not shown) thereby providing good evidence for only two contributing species. Similar results were obtained with data acquired

using the other peptides. Hence, distortions introduced by potential multiple affinity equilibria were considered to be small. This was further emphasised by the observation that determinations of values of K_a were independent of the wavelength used. For instance, K_a values determined for the B_{amph} peptide were independent of analysis wavelength (to within experimental error) over the range 500–580 nm, and the same value (again within experimental error) was obtained when the analysis was conducted using the total integrated fluorescence over the range 500–580 or 450–580 nm. This was also true of the other peptides too thereby providing evidence for the spectroscopic and thermodynamic uniformity of the groEL-binding sites occupied by individual bound peptides. Given this broad agreement between theory and experiment, we suggest that deviations from the assumptions made to derive expression (1) are sufficiently small to enable K_a, determined by experiment, to be equated to $K_{a,1}$ in expression (14) within the limits of experimental error. Therefore both binding data and derived thermodynamic parameters are representative of the first binding equilibrium in which peptide interacts with groEL.

Initially, the interactions of all five *N*-dansyl peptides, dansylglycine and dansylamide with groEL and three control proteins (*i.e.* HSA, DNase and lysozyme) were investigated (Table 1) to demonstrate that the assay procedure would provide physically meaningful information. Of the four proteins, only HSA showed a measurable affinity for dansylglycine whilst the other three, including groEL, did not. GroEL was also found not to interact with dansylamide. These results indicated that the *N*-dansyl group fluorophore was not itself interacting significantly with groEL and that the observed interactions of the *N*-dansyl peptides with groEL were driven by the peptide sequences alone. In contrast, the strength of the interaction between HSA and dansylglycine suggested that the observed interactions of HSA with the *N*-dansyl peptides were probably caused by interaction of fluorophore with the protein. Gratifyingly, the observed dissociation constant, K_d, of dansylglycine from HSA (for which *n* is known to be 1) was found to agree reasonably well with a published value[16] (Table 1) providing some evidence for the quantitative accuracy of our assay procedure. Of the four proteins studied, groEL was found to be unique in its ability to interact with the peptide sequence of the *N*-dansyl peptides, which is perhaps not surprising in view of its recognised function as a general molecular chaperone. Attempts were made to carry out competition experiments in which binding constants of *N*-dansyl peptides were measured in the presence of unlabelled B_{amph} peptide. In this way, we hoped to determine whether or not the various peptides were interacting with the same binding sites. The results were however somewhat disappointing. Generally speaking, increases in K_d values, consistent with same site competition, were not found to exceed the experimental error of the K_d values even at unlabelled B_{amph} peptide/*N*-dansyl peptide mol ratios of 100:1 (higher concentrations of competitor peptide were not tried owing to the likelihood of significant peptide self-association effects). This suggests that the number of groEL peptide binding sites, *n*, must be too large for there to be significant direct binding competition at any one binding site. Therefore, we cannot say definitively whether or not all four groEL-interacting peptides (*i.e.* B_{amph}, A_{amph}, N_{amph} and B_{hphil}) are binding at the same type of sites on groEL. However, in the case of all four peptides, the dansyl group fluorescence maxima, λ_{max}, at the 'saturation' point of the binding isotherms, were found to be within the spectrometer bandwidth (5 nm) of each other and therefore independent of the identity of the peptide. Since these maxima are a result of the polarity and rigidity of the local environment in which the dansyl chromophore is placed, then all the peptide binding site environments must at least be broadly similar.

Having established the utility of the assay system to investigate the interaction of peptides with groEL, the effects of ionic strength (Fig. 5) and temperature (Fig. 6) on the interaction of the five *N*-dansyl peptides with groEL were systematically analysed in order to define the forces involved and their relative importance to groEL peptide/protein molecular recognition. It is conceivable that ionic strength changes may alter peptide binding modes owing to the fact that salts are known to enhance the exposure of hydrophobic surfaces in groEL.[22] However, the fluorescence maxima, λ_{max}, at the 'saturation' point of the binding isotherms, were found to be within the spectrometer bandwidth (5 nm) of each other and therefore independent of ionic strength, suggesting that peptide binding modes were not significantly changing. The polar, acidic sequence A_{hphil} was unable to interact with groEL under any conditions (Table 1, Figs. 5 and 6). By contrast, the amphiphilic, acidic sequence $A_{amph}$was able to interact significantly but only after the ionic strength had exceeded 1.0 mol kg^{-1} [Table 1, Fig. 5(*a*)], at which point there was a measurable K_d which steadily decreased with increasing ionic strength. At 1 M $(NH_4)_2SO_4$, the interaction between the A_{amph} peptide and groEL was very slightly dependent on temperature over the range 10–42 °C (*i.e.* 283–315 K) as shown by the van't Hoff plot [Fig. 6(*a*)] and positive values of both standard enthalpy and entropy of binding (ΔH^{o}_{bind} and ΔS^{o}_{bind} respectively) were calculated (Table 2). Quite clearly, the presence of negative charge inhibited interaction with groEL, presumably because of electrostatic repulsion between groEL and the peptides probably owing to the fact that groEL itself is negatively charged (p*I* 4.5)[23] at neutral pH. At high ionic strength (>1.0 mol kg^{-1}), the electrostatic repulsion appears to have been minimised so that the A_{amph} peptide was able to bind. The involvement of hydrophobic interactions is suggested by the increase in binding affinity with increasing ionic strength [Fig. 5(*a*)], together with the small unfavourable enthalpy change and the large, positive entropy of binding (Table 2) which are consistent with the release of water of hydration from the binding interface; one characteristic of the hydrophobic effect.[24] Further evidence for hydrophobic interactions was obtained by fitting the A_{amph} peptide van't Hoff plot [Fig. 6(*a*)] to a truncated form of the integrated van't Hoff eqn. (17).[25] There are sufficient data points to

$$\ln K_a = a + b(1/T) + c \ln T \qquad (17)$$

suggest a slight positive curvature in the data set which could be fitted using eqn. (17) with the result that a $\Delta C_{p\ bind}$ value of approx. −1 kJ K^{-1} mol^{-1} was derived using eqn. (18).

$$\Delta C_{p\ bind} = Rc \qquad (18)$$

It would be inappropriate to attach too much significance to the magnitude. However, a negative sign of $\Delta C_{p\ bind}$ is known to be indicative of hydrophobic interaction[26] and this value is therefore consistent with the other pieces of evidence.

The N_{amph} peptide behaved similarly to the A_{amph} peptide although the N_{amph} peptide was able to interact with groEL at much lower ionic strengths, presumably owing to the absence of negatively charged side chains in the sequence [Fig. 5(*a*)]. In common with the A_{amph} peptide, the K_d of interaction was found to decrease steadily with increasing ionic strength. Moreover, both the van't Hoff plot [Fig. 6(*a*)] and the thermodynamic parameters ΔH^{o}_{bind} and ΔS^{o}_{bind} associated with the N_{amph} peptide at low ionic strength (Table 2) are similar to those of the A_{amph} peptide measured at high ionic strength. Therefore, the interactive behaviour of the N_{amph} peptide at low ionic strength is probably similar to that described previously for the A_{amph} peptide at high ionic strength.

The interactive behaviour of the B_{hphil} and B_{amph} peptides is more complex than that of the other three. The B_{hphil} peptide was found to interact significantly under conditions of low ionic strength (Table 1) but as soon as the ionic strength was increased above 0.02 mol kg^{-1}, this interaction became too

weak to measure [Fig. 5(*a*)]. The van't Hoff plot [Fig. 6(*a*)] was only linear over the narrow temperature range 30–42 °C (*i.e.* 303–315 K). Values of both ΔH°_{bind} and ΔS°_{bind} were calculated from this linear region (Table 2) but it is difficult to attach too much significance to these results. Nevertheless, the sensitivity of the interaction between the B_{hphil} peptide and groEL to ionic strength does suggest that attractive electrostatic forces dominate the interaction which is corroborated by the calculated large positive values of ΔH°_{bind} and ΔS°_{bind} (Table 2) consistent with a binding process in which extensive water of hydration is released from solvent cages surrounding charged groups.

The B_{amph} peptide was found to interact significantly with groEL over the complete range of ionic strength [Fig. 5(*a*)] but the K_d was observed to vary in a complex fashion which was found to be qualitatively similar when $MgCl_2$ was exchanged for $(NH_4)_2SO_4$ [Fig. 5(*b*)]. At low ionic strength, the interaction with groEL was very temperature dependent and from the linear van't Hoff plot [Fig. 6(*a*)] large positive values of ΔH°_{bind} and ΔS°_{bind} were calculated (Table 2). These thermodynamic parameters (Table 2) are similar to those of the B_{hphil} peptide, and are consistent with an interaction with groEL based almost exclusively on electrostatic attraction. However, as ionic strength is increased the observed fall in the large positive value of ΔH°_{bind} (Table 3), the reduced temperature dependency of K_a [Fig. 6(*b*)] and the gradual decrease in K_d with increasing ionic strength (above an ionic strength of 1.0 mol kg^{-1}) [Fig. 5(*a*)], indicate that the forces of electrostatic interaction are being superceded by hydrophobic interactions, similar to those which govern the association of N_{amph} and A_{amph} peptides with groEL. Nevertheless, since both ΔH°_{bind} and ΔS°_{bind} (Tables 2 and 3) remain larger positive values than those for either the N_{amph} or A_{amph} peptide, then an electrostatic interaction probably persists even at high ionic strength. Certainly, the B_{amph} peptide van't Hoff plots [Fig. 6(*b*)] show sufficient linearity over the fixed temperature range (283–315 K) to suggest that $\Delta C_{p\ bind}$ is almost zero. Therefore, the negative contribution to $\Delta C_{p\ bind}$, resulting from hydrophobic interactions,[26] is probably being supplemented by a positive contribution from electrostatic interactions resulting from dehydration of the protein interface and release of electro-stricted water.[27] Attempts were made to fit the B_{amph} peptide van't Hoff plots [Fig. 6(*b*)] with the integrated van't Hoff equation (17).[25] Although the data sets are not sufficient for accurate quantitative fitting, small, negative values of $\Delta C_{p\ bind}$ (approx. -0.3 kJ K^{-1} mol^{-1}) were derived using eqn. (18) which appear to be consistent with the above interpretation.

Conclusions

To what extent may these results be generalised to understand the processes of molecular recognition and binding of unfolded substrate proteins by groEL? It would be premature to derive sweeping generalisations about groEL molecular recognition on the basis of these studies with five different but related peptides, especially since the peptides were designed with an amphiphilic α-helix motif in mind and it is now known that peptide/protein interaction with groEL does not rest exclusively on such a motif.[28] However, it is well known that groEL will promiscuously associate with many different unfolded protein substrates,[29] underlining the fact that recognition of an unfolded protein by groEL is almost certainly not a phenomenon determined by specific amino acid sequences. Rather groEL is most probably making use of general structural features common to all unfolded proteins in order to bind so many different substrates. The five peptides studied here (Fig. 2) were designed and synthesised as systematic variants of each other in terms of their patterns of charge and hydrophobicity and could therefore be regarded as peptide mimics of a range of unfolded protein substrates. Certainly, under the optimal appropriate conditions, the apparent dissociation constants determined for the interaction of these peptides with groEL (Table 1, Figs. 5 and 6) are within two orders of magnitude of dissociation constants determined for the interaction of unfolded proteins with groEL.[14,30] This does not seem unreasonable in view of the fact that unfolded proteins presumably interact with groEL through several physically different sites and binding should be at least additive. Therefore, accepting that the five *N*-dansyl peptides used in our studies have some credibility as peptide mimics of larger unfolded proteins, then some new conclusions can be drawn about the general forces, and therefore the general structural characteristics, needed to bring about association between groEL and a substrate protein.

The importance of hydrophobic interactions for promoting the binding of unfolded or partially unfolded protein substrates to groEL is established[31,32] and strongly supported by the X-ray crystal structure of groEL which shows a high density of hydrophobic residues on the inside surface of the flexible apical domain, facing the central channel,[4] where substrate protein is known to bind.[3] However, the concurrent importance and relevance of electrostatic interactions is less well established. In the work reported above, of the five peptides studied only the amphiphilic N_{amph} and B_{amph} peptides were able to associate with groEL to a measurable extent at physiologically relevant ionic strengths (*i.e.* approx. 0.15 mol kg^{-1})[33] whilst the exclusively polar or anionic peptides A_{hphil}, B_{hphil} and A_{amph} were unable to interact. Moreover, the thermodynamic parameters measured (Tables 2 and 3) for the interaction of N_{amph} and B_{amph} peptides suggest that their binding interactions, at physiologically relevant ionic strengths, involved primarily hydrophobic interactions. However, the B_{amph} peptide, which interacted the most strongly, appeared to benefit from supplementary electrostatic interactions. These results suggest that positively charged amino acid residues can be helpful in augmenting binding to groEL through the provision of attractive electrostatic interactions. Furthermore, our studies with the A_{amph} peptide demonstrate that negatively charged amino acid residues can completely overwhelm short-range hydrophobic interactions at physiologically relevant ionic strengths, with binding only possible if the ionic strength is high enough to attenuate the electrostatic repulsion to groEL. Hence our data support the notion that whilst a principal means of interaction between groEL and substrate is certainly hydrophobic, electrostatic effects can modulate or overwhelm this interaction. Itzhaki *et al.*[34] have very recently published evidence, from studies on the refolding of chymotrypsin inhibitor 2 (CI-2) mutants in the presence of groEL, which provides direct support for all of these conclusions. Additional support is also provided by observations made with other groEL-interacting proteins and peptides.[35]

Some studies have suggested that an early folding intermediate of a protein substrate is optimal for recognition and binding by groEL[9,30,36] which could correspond to a molten globule state[32,37] although late folding intermediates are reported to be recognised and bound as well.[38] Where bound states of substrate proteins have been directly characterised, they appear to vary from molten globule[39] to a more native-like state in character.[40] In any event, our results suggest that within the structure of a partially folded protein substrate, amino acid residue sequences (or three-dimensional arrays) combining hydrophobic residues with either positively charged and/or polar neutral residues should interact with groEL whilst sequences (or arrays) which are exclusively polar or negatively charged will not. If we attempt to discriminate generally between factors which may promote recognition of substrate by groEL and factors which govern the strength of substrate binding to groEL, then we would propose that negatively charged amino acid residues are primary features of a partially folded substrate protein which act to discourage recognition whilst positively charged residues promote recognition, as well as contributing to binding strength through favourable electrostatic

interactions. The role of positively charged amino acid residues might then be to guide the substrate towards the apical domain binding site by electrostatic attraction, before hydrophobic interactions can take effect, in analogy to the way positively charged mitochondrial signal sequence peptides are thought to be recognised and interact with negatively charged mitochondrial membranes.[41]

In summary, the results described in this paper suggest that although hydrophobic interactions are central to the interaction between groEL and substrate proteins, electrostatic interactions are also important and can contribute to the strength of interaction as well as assisting in the recognition of unfolded protein substrates.

Acknowledgements

We thank the BBSRC, The Royal Society and Roche Products Ltd for financial support. T. C. O. acknowledges the support of the Association of Commonwealth Universities. We would also like to thank Professor Ben Selinger, Department of Chemistry, Australian National University, Canberra for the loan of a copy of the Markov 4.0.3 Kinetics Simulator program.

References

1 (*a*) R. W. Hendrix, *J. Mol. Biol.*, 1979, **129**, 375; (*b*) G. N. Chandrasekhar, K. Tilly, C. Woolford, R. Hendrix and C. Georgopoulos, *J. Biol. Chem.*, 1986, **261**, 12 414; (*c*) A. Azem, M. Kessel and P. Goloubinoff, *Science*, 1994, **265**, 653; (*d*) M. Schmidt, K. Rutkat, R. Rachel, G. Pfeifer, R. Jaenicke, P. Viitanen, G. Lorimer and J. Buchner, *Science*, 1994, **265**, 656; (*e*) A. Engel, M. K. Hayer-Hartl, K. N. Goldie, G. Pfeifer, R. Hegerl, S. Müller, A. C. R. da Silva, W. Baumeister and F.-U. Hartl, *Science*, 1995, **269**, 832.

2 H. R. Saibil, D. Zheng, A. M. Roseman, A. S. Hunter, G. M. F. Watson, S. Chen, A. auf der Mauer, B. P. O'Hara, S. P. Wood, N. H. Mann, L. K. Barnett and R. J. Ellis, *Curr. Biol.*, 1993, **3**, 265.

3 S. Chen, A. M. Roseman, A. S. Hunter, S. P. Wood, S. G. Burston, N. A. Ranson, A. R. Clarke and H. R. Saibil, *Nature*, 1994, **371**, 261.

4 K. Braig, Z. Otwinowski, R. Hegde, D. C. Boisvert, A. Joachimiak, A. L. Horwich and P. B. Sigler, *Nature*, 1994, **371**, 578.

5 J. F. Hunt, A. J. Weaver, S. J. Landry, L. Gierasch and J. Deisenhofer, *Nature*, 1996, **379**, 37.

6 A. D. Miller, K. Maghlaoui, G. Albanese, D. A. Kleinjan and C. Smith, *Biochem. J.*, 1993, **291**, 139.

7 (*a*) R. Zahn and A. Plückthun, *Biochemistry*, 1992, **31**, 3249; (*b*) N. A. Ranson, N. J. Dunster, S. G. Burston and A. R. Clarke, *J. Mol. Biol.*, 1995, **250**, 581.

8 R. A. Staniforth, A. Cortes, S. G. Burston, T. Atkinson, J. J. Holbrook and A. R. Clarke, *FEBS Lett.*, 1994, **344**, 129.

9 T. E. Gray and A. R. Fersht, *J. Mol. Biol.*, 1993, **232**, 1197.

10 (*a*) G. S. Jackson, R. A. Staniforth, D. J. Halsall, T. Atkinson, J. J. Holbrook, A. R. Clarke and S. G. Burston, *Biochemistry*, 1993, **32**, 2554; (*b*) M. J. Todd, P. V. Viitanen and G. H. Lorimer, *Science*, 1994, **265**, 659.

11 J. Martin, M. Mayhew, T. Langer and F.-U. Hartl, *Nature*, 1993, **366**, 228.

12 J. S. Weissman, C. M. Hohl, O. Kovalenko, Y. Kashi, S. Chen, K. Braig, H. R. Saibil, W. A. Fenton and A. L. Horwich, *Cell*, 1995, **83**, 577.

13 (*a*) J. S. Weissman, Y. Kashi, W. A. Fenton and A. L. Horwich, *Cell*, 1994, **78**, 693; (*b*) R. Zahn, C. Spitzfaden, M. Ottiger, K. Wüthrich and A. Plückthun, *Nature*, 1994, **368**, 261; (*c*) H. Taguchi and M. Yoshida, *FEBS Lett.*, 1995, **359**, 195; (*d*) G. Tian, I. E. Vainberg, W. D. Tap, S. A. Lewis and N. J. Cowan, *J. Biol. Chem.*, 1995, **270**, 23910; (*e*) F. J. Corrales and A. R. Fersht, *Proc. Natl. Acad. Sci., USA*, 1995, **92**, 5326; (*f*) R. Hlodan, P. Tempst and F.-U. Hartl, *Nature Struct. Biol.*, 1995, **2**, 587.

14 R. A. Staniforth, S. G. Burston, T. Atkinson and A. R. Clarke, *Biochem. J.*, 1994, **300**, 651.

15 H. Edelhoch, *Biochemistry*, 1967, **6**, 1948.

16 C. F. Chignell, *Mol. Pharmacol.*, 1969, **5**, 244.

17 H. A. Benesi and J. H. Hildebrand, *J. Am. Chem. Soc.*, 1949, **71**, 2703.

18 K. A. Connors, *Binding Constants: The Measurement of Molecular Complex Stability*, Wiley, New York, 1987.

19 L. Brand and J. R. Gohlke, *Ann. Rev. Biochem.*, 1972, **41**, 843.

20 S. J. Landry and L. M. Gierasch, *Biochemistry*, 1991, **30**, 7359.

21 J. S. Coleman, L. P. Varga and S. H. Mastin, *Inorg. Chem*, 1970, **9**, 1015.

22 P. M. Horowitz, S. Hua and D. L. Gibbons, *J. Biol. Chem.*, 1995, **270**, 1535.

23 H. F. Rosenberg, S. J. Ackerman and D. G. Tenen, *J. Biol. Chem.*, 1993, **268**, 4499.

24 G. C. Kresheck, L. B. Vitello and J. E. Erman, *Biochemistry*, 1995, **34**, 8398.

25 J. C. Lee and S. N. Timasheff, *Biochemistry*, 1977, **16**, 1754.

26 J. M. Sturtevant, *Proc. Natl. Acad. Sci., USA*, 1977, **74**, 2236.

27 J. H. Ha, R. S. Spolar and M. T. Record Jr., *J. Mol. Biol.*, 1989, **209**, 801.

28 M. Schmidt and J. Buchner, *J. Biol. Chem.*, 1992, **267**, 16829.

29 P. V. Viitanen, A. A. Gatenby and G. H. Lorimer, *Protein Science*, 1992, **1**, 363.

30 J. P. Hutchinson, T. S. H. El-Thaher and A. D. Miller, *Biochem. J.*, 1994, **302**, 405.

31 (*a*) G. Richarme and M. Kohiyama, *J. Biol. Chem.*, 1994, **269**, 7095; (*b*) W. A. Fenton, Y. Kashi, K. Furtak and A. L. Horwich, *Nature*, 1994, **371**, 614; (*c*) R. Zahn, S. E. Axmann, K.-P. Rücknagel, E. Jaeger, A. A. Laminet and A. Plückthun, *J. Mol. Biol.*, 1994, **242**, 150; (*d*) Z. Lin, F. P. Schwarz and E. Eisenstein, *J. Biol. Chem.*, 1995, **270**, 1011.

32 M. K. Hayer-Hartl, J. J. Ewbank, T. E. Creighton and F.-U. Hartl, *EMBO J.*, 1994, **13**, 3192.

33 J. F. Eccleston, K. J. M. Moore, L. Morgan, R. H. Skinner and P. N. Lowe, *J. Biol. Chem.*, 1993, **268**, 27012.

34 L. S. Itzhaki, D. E. Otzen and A. R. Fersht, *Biochemistry*, 1995, **34**, 14581.

35 (*a*) T. E. Gray, J. Eder, M. Bycroft, A. G. Day and A. R. Fersht, *EMBO J.*, 1993, **12**, 4145; (*b*) C. W. Dessauer and S. G. Bartlett, *J. Biol. Chem.*, 1994, **269**, 19766; (*c*) J. R. Mattingly, Jr., A. Iriarte and M. Martinez-Carrion, *J. Biol. Chem.*, 1995, **270**, 1138.

36 A. Okazaki, T. Ikura, K. Nikaido and K. Kuwajima, *Nature Struct. Biol.*, 1994, **1**, 439.

37 G. C. Flynn, C. J. M. Beckers, W. A. Baase and F. W. Dahlquist, *Proc. Natl. Acad., Sci., USA*, 1993, **90**, 10826.

38 (*a*) H. Lilie and J. Buchner, *Proc. Natl., Acad. Sci., USA*, 1995, **92**, 8100; (*b*) K. E. Smith and M. T. Fisher, *J. Biol. Chem.*, 1995, **270**, 21517.

39 C. V. Robinson, M. Groß, S. J. Eyles, J. J. Ewbank, M. Mayhew, F.-U. Hartl, C. M. Dobson and S. E. Radford, *Nature*, 1994, **372**, 646.

40 J. P. Hutchinson, C. Smith, T. S. H. El-Thaher and A. D. Miller, in *Perspectives on protein engineering*, ed. M. J. Geisow, Mayflower Worldwide, Birmingham, UK, 1995, pp. 287–291.

41 Y. Wang and H. Weiner, *Biochemistry*, 1994, **33**, 12 860.

Paper 6/04880C
Received 11*th July* 1996
Accepted 10*th September* 1996